

Associating Molecular Physicochemical Properties with Ionization Efficiency for Compounds in Aprotic, Polar Solvent Using Field-free and Field-enabled cVSSI Techniques

Kinkini Jayasundara and Stephen J. Valentine

C. Eugene Bennett Department of Chemistry, West Virginia University, Morgantown WV 26506

Abstract

The relationship between separate molecular physicochemical properties and ionization efficiency has been investigated for the new ionization technique capillary vibrating sharp-edge spray ionization (cVSSI). Intensity values have been recorded for both positively- and negatively-charged ions arising from various compounds in the aprotic, polar acetonitrile (ACN) solvent environment. These have been recorded for field-free cVSSI as well as field-enabled cVSSI and compared to results obtained from standard ESI. In general, the strongest correlating factors include the logarithm of the octanol/water partition coefficient ($\log P$) and the compound proton affinity (PA) in both positive and negative ion mode. This is contrasted with results for the polar, protic solvents water and methanol where the log of the base dissociation constant (pK_b) often produced the strongest correlation. The results suggest that, in the absence of abundant protonating reagent, pre-formed ions do not govern the ionization process for samples in the ACN solvent systems. Another notable result is the increased ion signal levels observed for the majority of the ions in positive ion mode upon their production by a field-free source; that is, remarkably, the application of a DC voltage to the solution serves to decrease the overall ion signal level. Overall, it appears that, regardless of whether or not ions are produced by the charged residue model or the ion evaporation model, gas-phase proton transfer reaction is the major process by which they are produced.

Email: stephen.valentine@mail.wvu.edu

Introduction

Mass spectrometry is one of the most versatile analytical techniques used for characterizing a broad range of samples, providing the mass-to-charge ratios (m/z) for gas-phase ions of various compounds. With the introduction of the soft ionization electrospray ionization (ESI)¹ and matrix-assisted laser desorption ionization (MALDI)² in the 1980s, there was a rapid proliferation of new ionization sources such as atmospheric pressure MALDI³, micro- and nanospray ionization^{4, 5}, desorption electrospray ionization (DESI)⁶, direct analysis in real time (DART)⁷, and atmospheric pressure chemical ionization (APCI)⁸. Due to the high utility of mass spectrometry applications in fields like chemical/biological warfare agent detection, forensic investigation, on-site metabolomics identification, and atmospheric toxic particle detection, the need for miniaturized and field-portable mass spectrometers has arisen^{9, 10, 11, 12, 13}. The need for in-situ and field analyses by MS has coincided with the development of various field-free ionization techniques such as sonic spray ionization (SSI)¹⁴, zero-voltage paper spray ionization (PSI)¹⁵, surface acoustic wave nebulization (SAWN)¹⁶, solvent assisted inlet ionization (SAII)¹⁷ and ultrasonication-assisted spray ionization¹⁸.

Recently, Li and coworkers introduced a new, field-free spray-based ionization technique called vibrating sharp-edge spray ionization (VSSI)¹⁹. This unique ion source only requires a vibrating substrate containing a sharp edge. When a liquid sample is placed at the edge of a vibrating microscope slide and a RF voltage is applied to an attached piezoelectric transducer, the vibrating (~ 100 kHz) substrate produces a plume of micrometer-sized droplets emanating from the sharp tip of the slide. In the initial work, it VSSI has been shown to produce ESI-like ions even though no external electric field was utilized. The later addition of a capillary segment/tip to the glass slide presented another form for a sharp edge for efficient introduction of a sample-infused plume to a mass spectrometer inlet; this has been termed capillary vibrating sharp-edge spray ionization (cVSSI)²⁰. Finally, the application of a DC voltage to the solution infused through a cVSSI device (field-enabled cVSSI) provided an enhanced means of ion production. Remarkably, a ~ 10 to 100-fold ion signal enhancement in MS analyses in negative ion mode compared to ESI has been demonstrated²¹. Modest improvements (typically 5-fold) have also been observed for positive ion mode experiments. That said, because cVSSI can be conducted without the application of a voltage to the solution, the generated plume may exhibit some similarities to droplets produced by SSI, SAII, SAWN, and Zv-PSI. That said, it is here stressed that the plume generated by VSSI and cVSSI results from a unique, mechanical vibration process that provides advantages with regard to ease of on-line coupling, robust function over a wide range of infused flow rates, and reduced footprint due to very low power requirements. The very fact that such differences exist could suggest that the droplet plume produced by VSSI and cVSSI has unique characteristics that can be exploited/tailored for MS analyses.

Over the years, much research effort has been expended to improve the ionization efficiency of new spray-based ionization techniques for MS analyses. For example, the use of heated transfer tubes and bath gas facilitated ion desolvation in SAI and droplet-assisted inlet ionization⁷⁻²². The advantages of using a carbon nanotube (CNT)-impregnated paper surface in field-free PSI²³ and incorporating microchips and microfluidics chips in sonic spray ionization to enhance ionization efficiency have also been shown²⁴⁻²⁵. One area of research that has lagged in field-free ion source studies has been the determination of the roles of analyte physicochemical properties on the overall ionization efficiency as well as ionization effects resulting from different solvent systems. Because of the potential for field-free ionization sources in the various fields mentioned above, the research gap should be filled with robust studies seeking to elucidate such roles for these techniques.

Over the years, several large-scale studies have sought to correlate specific physicochemical properties with ionization efficiency by ESI²⁶⁻³¹. Here, studies show that the log of the base dissociation constant (pK_b) significantly correlated with the ionization efficiency in small molecule analysis.²⁷⁻²⁹ Other studies have shown that different solvent conditions such as pH, polarity, and volatility influence ion signal levels in ESI.³⁰⁻³¹ In an early study, Kebarle and coworkers reported that the high methanol content in a mixture of water and methanol gave rise to an enhancement in signal intensity of cocaine ions produced by ESI.³² In separate studies it was shown that by increasing the volume ratio of organic solvent in methanol/water and acetonitrile/water systems incremental changes in ion intensities of organic compounds could be achieved; as a general comparison, the optimum ion intensities for acetonitrile/water solvents were observed at lower proportions of organic component than for the methanol solvent system.³³ A similar observation was observed by Schneider *et al.* where it was found that the ion current was suppressed when 100% acetonitrile was used as the mobile phase in condensed-phase separations.³⁴ In contrast, Takayama and coworkers showed that when amino acids were examined in negative ion mode under different solvent compositions of methanol and acetonitrile, higher ion signals were obtained with higher acetonitrile content.³⁵ They proposed this may be due to a lower vaporization enthalpy for acetonitrile compared to methanol. In summary, these studies suggest that increased ion signal intensity is due to an increase in the production efficiency of small droplets during the ESI process accomplished by a decrease in the surface tension and vaporization enthalpy of the solution system.

Another novel, voltage-free ionization technique employing a vibration tip has shown that increasing the methanol content to 100% in a water/methanol buffer system resulted in a significant ion signal enhancement compared to lower methanol content solutions.³⁶ Thus, the solvent effect on ionization efficiency differ between high voltage ionization techniques like ESI and voltage-free techniques. Such differences are also altered based on the voltage polarity (positive or negative) utilized in experiments. It is therefore important to compare the solvent effects for small molecules for different ionization techniques (high voltage and field-free) are

in both positive and negative mode. To highlight the importance of such studies, consider that the new knowledge will be beneficial for LC/MS studies allowing the selection of the optimum solvent conditions when coupling to different ionization techniques.

The facile manner with which a DC voltage can be coupled with cVSSI make it an ideal source to perform studies seeking to understand the effects of solvent composition and molecular properties on ionization efficiency. Here, the same emitter tip can be used for voltage-free cVSSI, field-enabled cVSSI, and capillary ESI without introducing confounding factors such as a nebulization gas as is associated with current state-of-the-art ESI sources. Indeed, prior work explored the association of three molecular properties (proton affinity, solution base dissociation constant, and polarity) with ion intensities for compounds analyzed by field-free and field-enabled cVSSI.³⁷ The results were compared with ESI using the same flow rates and emitter tips.

The work reported here extends the study of ion formation by cVSSI techniques to include the new solvent systems of acetonitrile as well as acetonitrile:water (95:5). The work focuses on the influence of the aprotic environment on ionization efficiency in both positive and negative ion mode. A motivation for this study is the fact that acetonitrile is used extensively in condensed-phase separations (e.g., HILIC and reversed-phase LC) employed in metabolomics analyses. Correlation studies involving the physiochemical properties $\log pK_b$, $\log P$, and proton affinity (PA) and ion intensity have been conducted in both positive and negative ion mode. These experiments were conducting using voltage-free cVSSI, field-enabled cVSSI, and ESI. Notable differences are observed compared to the prior work examining protic solvent systems (water and methanol). Here, pK_b less frequently correlates with ionization efficiency even when employing a DC voltage. Additionally, differences are observed in positive ion mode compared to negative ion mode; for example, for the former, both $\log P$ and PA appear to be most associated with ionization efficiency while for negative ion mode, the primary association is PA. The results are discussed with regard operational ionization mechanisms under different solvent compositions and electric field conditions.

Experimental

Ionization device fabrication. Pulled-tip capillary emitters were obtained using a laser puller (Sutter Instrument Co, Model P-2000, Novato CA, USA) and fused silica (100 μm ID \times 360 μm ID). Emitter tip diameters were examined by microscope to ensure that the tip sizes were ~ 25 to 30 μm . Previous work demonstrated that droplet size distribution under field-free cVSSI for aqueous solutions is $17.5 \pm 5.6 \mu\text{m}^{20}$. cVSSI and ESI devices were fabricated as described previously³⁷. The VSSI devices were constructed by attaching a piezoelectric transducer (Murata) to a microscope glass slide using epoxy-based superglue (Devcon). Pulled emitter tips were glued to each microscope slide at the distal end using an angle of $\sim 60^\circ$. The sample

solutions were infused through a syringe connected to PTFE tubing. The opposite end of the PTFE tubing was slip fit over the cVSSI emitter. In field-enabled cVSSI and ESI, high voltage was supplied to the solvent by connecting to a Pt wire that punctured into the PTFE tubing near the emitter tip connection.

Reagents and Sample Preparation. For the experiments described here, 18 compounds for positive ion mode and 14 compounds for negative ion mode studies were used. Many of the compounds overlapped with those used in the previous study examining the physiochemical properties correlation in the polar, protic solvents of methanol and water. The compounds N-ethylaniline, cimetidine, phenylethylamine, acetaminophen, N-N dimethylethyldiamine, 4-methoxyaniline, N-N dimethylbenzylamine, atropine, methyltriazinane c, 4-aminobenzoic acid, N-methylbenzylamine, 3-aminopyridine, tetracine, metronidazole, DADLE, trans-1,2 diaminocyclohexane, alpha-ketoglutaric acid, 2,4-dimethylphenol, phenol, p-cresol, benzoic acid, pentachlorophenol, MCPA, dichloropropanol, captopril, acetylsalicylic acid, and 4-nitrophenol were purchased from Thermo Fisher Scientific (Pittsburgh, PA, USA) and used without further purification. Tables S1 and S2 in the Supporting Information section show the structures of the compounds and their molecular weights, log P , pK_b , and PA values. The majority of the PA values were obtained from the NIST Chemistry WebBook; for the compounds not included on the NIST website, PA values were calculated using the Gaussian 09 software suite. pK_a values in acetonitrile were computed using the empirical conversion proposed previously.³⁸ Stock solutions of each compound were prepared by dissolving 1 mg of each compound in 1 ml of solvent. Two different solvent systems were investigated, neat acetonitrile and a solvent mixture of acetonitrile and water in a 95:5 ratio (95% acetonitrile).

Mass Spectrometry Data Collection. The experiments were carried out on an Orbitrap mass spectrometer (Q Exactive, ThermoFisher). The commercial ionization source was removed from the mass spectrometer, and the system software was externally triggered. The cVSSI device was placed directly in front of the MS inlet at a distance of ~ 1 cm throughout the data collection. Data were collected under field-free cVSSI, field-enabled cVSSI, and ESI conditions. For the two cVSSI conditions, the glass slide was vibrated using an RF voltage of ~ 10 V_{pp} at a frequency of ~ 92 to 94 kHz (square wave). In both field-enabled cVSSI and ESI, a DC voltage of ± 2 kV was utilized. Separate experiments were carried out with different sets of molecules for positive ion mode and negative ion mode experiments on the mass spectrometer. The temperature of the ion transfer tube was maintained at 275 °C for all experiments. Data were collected for 30 s over a mass-to-charge ratio (m/z) range of 50-750.

Data Analysis. For all comparisons, ion signal intensities were obtained for each compound using the Xcalibur software suite (ThermoFisher). Linear regression was performed using the Excel software suite (Microsoft, Redmond, CA) for single parameter correlations of peak intensity versus physiochemical property of the molecules. The R^2 values of each separate analysis were compared.

Multiple regression analysis was performed using the regression IBM SPSS Statistics 25 software suite using each analyte's peak intensity and physicochemical properties. In multiple regression analysis, the three physicochemical properties mentioned above were designated as independent variables and peak intensities were designated as the dependent variables. Each property's relative association with the degree of ionization (ion intensity) was compared using the beta coefficient values from the multiple regression analysis. The coefficients and their associated significances are listed in Table 1 and 2 for each ionization mode and solvent system.

Results and Discussion

Relative ion intensities for compounds in neat acetonitrile using positive ion mode. A total of 18 compounds have been examined for ion production from acetonitrile solutions. Here, field-free cVSSI as described previously³⁷ has been used initially to examine the relative ion signal levels produced in this operational mode. Figure 1 and Table S3 (a) show the ion intensity levels for the different compounds. Overall, when voltage-free cVSSI is employed in positive ion mode, the ion signal intensity values span a relatively wide range ($\sim 10^6$ to 10^8). Notably, the minimum and maximum value of this range is significantly greater than that obtained ($\sim 10^4$ to 10^5) in the prior studies for compounds in water solutions examined by field-free cVSSI. Additionally, the magnitude of the range is also moderately greater than that obtained for methanol studies ($\sim 10^5$ to 10^7). For the prior studies, the same solution flow rates, pulled-tip emitter sizes, distance to the mass spectrometer inlet, and instrumentation settings were used as described in the Materials and Methods section above. Admittedly, not all of the compounds are the same as those examined by water and methanol; however, there are 7 compounds that are the same and a similar diversity in terms of pK_b , $\log P$, and PA is captured in the 18 compounds studied here.

Upon applying a voltage to the infused acetonitrile samples while vibrating the cVSSI device (field-enabled cVSSI), the average ion signal intensities decreased slightly for most compounds (Figure 1). Exceptions to this observation are N-Ndimethylethyldiamine, benzamide, and metronidazole. When the vibration of the emitter tip is subsequently stopped (ESI only), a total of seven compounds show significantly decreased ion intensity levels while four exhibit increased ion signal levels (Figure 1). The six remaining compounds exhibit similar levels (field-enabled cVSSI versus ESI) of ion production. From the previous work, when methanol and water solutions were used under applied voltage conditions (field-enabled cVSSI and ESI), the same analyte compounds (4-methoxyaniline, N-ethylaniline, phenylethylamine, Methyltriazinamine c, N-methylbenzylamine, N-N-dimethylbenzylamine) have shown greater ion signal levels ($\sim 10^2$ on average) compared to the neat acetonitrile solvent system.

In summary, for positive ion mode analyses by field-free cVSSI of compounds in the polar, aprotic solvent acetonitrile, significant enhancements in ionization are observed when compared with results from polar protic solvents. Additionally, with the application of a DC voltage to the solution, notable changes in ion intensities are observed depending upon whether or not the emitter tip undergoes vibration. In comparison to the polar, protic solvents examined in the prior work, the ion intensity levels here are relatively depressed for both field-enabled cVSSI and ESI.

Relative ion intensities for compounds in acetonitrile(ACN):water (95:5) solutions using positive ion mode. Having noted that ion production is enhanced for polar protic solvent systems upon the application of voltage, experiments have been designed to examine the effect of a small addition of such solvent to the acetonitrile solution. To investigate the effect of increased protic solvent content on the ion signal levels, the same set of analyte compounds have been examined using an ACN:water (95:5) solvent system. All other instrumentation and data collection parameters are identical to those described for the neat acetonitrile experiments. Figure 2 and Table S3(b) shows the different ion intensity values obtained for the various compounds that are sprayed from this solution composition. In general, for field-free cVSSI, the ion intensity values do not change significantly (compared with neat ACN) ranging between 10^6 and 10^8 . Notable exceptions are N-N dimethylethyldiamine and benzamide where a significant increase and a decrease, respectively, are observed. Remarkably, the general ordering of ion intensities is preserved between the two different sample solution sets for field-free cVSSI.

The application of voltage to the ACN:water solution (Figure 2) generally results in increased ion intensity levels (compared with neat ACN – Figure 1) for many compounds. This is consistent with the increased ionization observed for identical compounds in water solution that occurs with the application of voltage³⁷. A notable exception is benzamide where the ion intensity levels decrease significantly for both field-enabled cVSSI and ESI.

Relative ion intensities for compounds in neat acetonitrile using negative ion mode. A total of 15 compounds have been examined for ion production from ACN solution in the negative ion mode studies. When field-free cVSSI is used to ionize the analyte molecules dissolved in neat ACN, the ion signal intensity values ranged between $\sim 10^{2.5}$ and $\sim 10^6$ as shown in Figure 3 and Table S4.a. These values represent the lowest ionization efficiency recorded for the acetonitrile studies presented here. In short, these varied compounds do not efficiently produce negatively charged ions from ACN solutions.

Upon utilizing the field-enabled conditions, ion signals are increased significantly (within the range of $\sim 10^6$ to 10^{10}) for both field-enabled cVSSI and ESI. Here it is noted that this behavior is exactly opposed to that observed in positive ion mode (Figure 1). In the positive ion mode studies, the field-free cVSSI generally provided the greatest ion production. In this case, the difference is more pronounced as multiple compounds exhibit $>10^3$ fold difference in ion intensity with the application of the DC voltage. Additionally, the ion intensities for field-enabled cVSSI and ESI are similar for most compounds and thus the same general ordering of ionization efficiency is preserved between the two methods (Figure 3). Notably, greater variability in ionization efficiency was observed for these two ionization methods in positive ion mode (Figure 1).

Relative ion intensities for compounds in acetonitrile(ACN):water (95:5) solutions using negative ion mode. When the 15 compounds used for negative ion mode studies are examined in an ACN solution containing 5% water, ionization efficiency for field-free cVSSI remains the lowest of the three techniques as shown in Figure 4 and Table S4.b. That is, the two methods employing a DC voltage provide the greatest ion signal levels. Notably, for field-free cVSSI only one compound shows a truly significant change; pentachlorophenol ion signal increases by nearly 3 decades. With the application of voltage, the ion signal levels are also similar to those observed for the neat ACN studies. One exception is the ion signal level obtained for acetylsalicylic acid where an increase of at least 2 decades is obtained for the 5% water solution (Figure 4).

Associating molecular physicochemical property with ion intensity in positive ion mode studies. It is instructive to consider the relationship of different physicochemical properties of analyte molecules and ion signal levels. Such efforts may be useful to obtain information about operative ionization mechanisms for the various techniques. Multiple regression analysis examines the correlations between ion signal levels (e.g., Figures 1-4) and the three distinct physiochemical molecular properties, pK_b , $\log P$, and PA . Table 1 and Table 2 show the beta coefficient values for each of the properties and their corresponding significance from the multiple regression analysis for data obtained from the samples in neat and 95% ACN, respectively.

For the experiments in which neat ACN solutions were used, no significant ($p < 0.05$) associations are observed with compound pK_b . This stands in stark contrast to the prior work in which pK_b correlated the most frequently for water and methanol solutions³⁷. For neat ACN, $\log P$ exhibits a significant correlation for all three ion source types. However, it is directly and indirectly correlated for field-free and applied voltage conditions, respectively. For the same solution, the largest significant correlation exists for PA for the experiments in which an electric field is utilized; for field-free cVSSI, this correlation is just outside the confidence interval ($p = 0.073$, Table 1). This is also very different than the prior results for methanol and

water where the pulled-tip emitter studies showed no significant correlation with PA for all three ionization sources.

Associating molecular physicochemical property with ion intensity in negative ion mode studies. Having noted the differences between molecular property correlations with intensity between the protic and aprotic solvent systems, it is useful to determine whether or not unusual behavior is observed when producing negatively-charged droplets. As indicated above, expanding the knowledge of factors contributing to negative ion production of different molecules by the various techniques could hold tremendous value for many different experiments. For example, consider ‘omics experiments in which quantitative determinations of nucleotides, carbohydrates, and fatty acids are desired. That is, the new knowledge from molecular property correlations could help to tailor ion source type (e.g., field-free cVSS) and solvent system to targeted compound analyses.

When the solvent is neat ACN, the largest correlating factor of significance is PA for all three ionization sources. In every case (field-free and field-enabled), PA is inversely correlated with ion intensity. In contrast to the positive ion mode studies, no significant correlation is obtained for $\log P$. Another deviation from the positive ion mode data is the observation of significant correlations with pK_b for both field-free and field-enabled cVSSI. These are both direct correlations.

When the solvent is ACN:water (95:5), the largest correlations of significance are also observed for PA . Also, as observed for neat ACN, these are inverse correlations. One difference when compared to the neat ACN is that $\log P$ is observed to provide significant correlation for field-free and field-enabled cVSSI but not for ESI. Finally, pK_b is observed to correlate in an inverse manner for ESI.

Ionization process considerations. Field-induced ionization processes like ESI have long shown strong correlations between pK_b and ion intensity for small molecules examined from polar, protic solvents like water and methanol.^{29 26 39} Several extensive studies have shown that other molecular properties such as $\log P$ and volatility of the analyte molecules can also correlate with ionization efficiency.^{30 40} Because so little is known about ionization from aprotic polar solvents, the studies reported here were pursued with the goal of determining the operative ionization processes for different source types. Above, the molecular property correlations with ionization efficiency for analytes in a polar, aprotic solvent were reported as well as the determination of how those correlations are subject to change upon adding an incremental amount of a polar, protic solvent (water) to the solutions. A question arises as to whether or not such correlations shed light on the type of ionization processes occurring for the different combinations of solvent system and ion source type. This is examined below.

It is widely accepted that the ionization of small molecules by ESI occurs via the ion evaporation mechanism (IEM) proposed by Iribarne and Thomson.^{41 42 43 44 45} In IEM, when

the field created by surface charge density on a droplet is sufficient to overcome forces associated with ion solvation, an analyte ion will be released to the gas phase environment.⁴⁶ Work performed by various research groups shows that the field-induced emission process is more efficient for the ionization of molecules having low pK_b (preformed ions in solution).^{27 47} This occurs as columbic interactions within the droplet cause the protonated species to locate near the droplet's surface. As further solvent evaporation events occur, a sufficiently strong field is formed to eject such preformed ions into the gas phase. So, this process is considered to be the primary method for ESI ion production of small molecules in protic solvent media. Additionally, it has been proposed that field-free ionization sources such as SSI produce ions via the charge residue model (CRM)⁴⁸ of ion production;¹⁴ here, molecules are retained in the droplets until the last vestiges of solvent desorb and charge is transferred to the analyte. Hence, in the absence of a protic solvent medium, analyte molecules may undergo different protonation processes and/or different methods of release into the gas phase.

Apart from pK_b , the influence of surface activity or hydrophobicity of the molecules has been shown to correlate with small-molecule ion signal intensities in ESI when analytes were sprayed from aqueous media.^{39 49 47 50} That said, Cech and coworkers reported that when the small molecules are sprayed from organic solvent like methanol there is no direct correlation between $\log P$ and ion signal intensity.²⁷ Consistent with this work was the prior cVSSI studies in which no significant association of $\log P$ and ion signal level was obtained for ESI of methanol solutions³⁷. Hence, the influence of molecule surface activity can be different depending on the solvent properties.

A remarkable feature of the work reported here is that even in the absence of a protic agent (neat ACN) both protonated and deprotonated ions are readily formed even in the absence of an applied voltage. One explanation could be that the residual ($\sim 0.05\%$) water in neat ACN may serve directly to produce H_3O^+ protonating reagent within the droplet. Another explanation can be extracted from the results of previous studies where the protonation of different molecules under ESI was not expected. Fenselau and coworkers detected protonated proteins upon being electrosprayed from highly basic (pH=10) solutions; there the solution basicity was adjusted using ammonia.⁵¹ Wang and Cole reported protonation of peptides and small proteins in very basic solvent conditions and named this phenomenon as the “wrong-way-round” method.⁵² Boyd and co-workers have shown strong protonation incidents for smaller analytes like amino acids similar to that reported for the “wrong-way-round” method⁵³ Zhou and Cook observed protonated caffeine from strong basic (ammonia) solutions and suggested this might result from an electric discharge-induced ionization process emanating from the ESI tip similar to atmospheric pressure chemical ionization (APCI). They suggested that this processes could account for much of the established “wrong-way-round” processes.⁵⁴

Having established that ionization processes can lead to ion formation that is not intuitive, it is instructive to consider the correlations in Tables 1 and 2 to consider this unusual ion formation

by cVSSI. For positive ion production by field-free cVSSI (Table 1), the strongest correlating factor is $\log P$. Here it may be argued that, in the absence of high charge density at the droplet surface, the more surface-active molecules will locate at the interface with the apolar gas-phase environment and are thus released from the droplet more readily. Comparatively, with the addition of voltage, the increased droplet surface charge would favor more polar species (or at least be less discriminating against). This may account for the inverse correlation with $\log P$ for field-enabled cVSSI and ESI (Table 1). Additionally, PA becomes the greatest correlating factor.

To consider why PA could be a factor in field-free ionization, it is instructive to further consider ion production using a “wrong-way-round” protonation process as proposed by Kebarle and Ho.^{55 56} It was suggested that, because the basic solutions were made with ammonia and NH_4^+ ions, the latter must be the major charge carriers on the droplet surface. They also suggest that multiple NH_4^+ ions could protonate the protein in a manner similar to proton transfer reaction in the gas phase. In this scenario, when analyte molecules such as proteins undergo the CRM, protonation may be expected to happen at the end stage as the last solvent components leave the protein-containing droplet. Similarly, protonation may occur for ions that go through the IEM when the analyte desorbs from the surface and represents a stronger base in the gas phase than NH_3 .

Although the above explanation, is consistent with the observation that PA correlates strongly with ion signal level for field-free cVSSI (Table 1), there exists an alternate scenario for gas-phase proton transfer. Boyd and co-workers have presented somewhat contradictory results. When basic amino acids like histidine were electrosprayed in a non-protic (tetramethylammonium hydroxide) basic solution, protonated amino acids, although unexpected, were observed.⁵³ For these types of scenarios, when there is not an abundant proton source in the solution phase, a discharged-induced ionization process may be possible as a result of the high voltage applied to the ESI tip.⁵⁴ Here, protonated solvent clusters would be generated in the gas phase similar to that described in the mechanism for atmospheric pressure chemical ionization (APCI) initiating from ambient species such as N_2 and O_2 . These protonated solvent clusters would then serve as reagent ions and undergo proton transfer reaction in the gas phase as explained by Kebarle and Ho. Notably, the introduction of the droplet plume produced by cVSSI into an electrical discharge region termed cVSSI-APCI, shows remarkable ionization efficiency⁵⁷. In the absence of a high electric field, alpha-particle irradiation of moist air can occur⁵⁸ and it can be argued that this process can be facilitated by the cVSSI tip vibration⁵⁹. Additionally, gamma irradiation can account for the production of ions which initiate the cascade responsible for production of protonated solvent clusters. Therefore, the above-mentioned discharged-induced ionization can be operative even with the field-free cVSSI technique.

When the water solvent is added to the ACN, the correlating factors remain relatively the same for positive ion mode (Table 1). A direct correlation between $\log P$ and ion intensity is observed with field-free cVSSI. This shifts to an inverse correlation for $\log P$ and the largest correlation for PA when a DC voltage is used for the other two ionization sources. Thus, it can be argued that molecule/ion release from the droplet and protonation is similar to that observed for positive ion production from neat ACN. That is, 5% water is not sufficient to shift the ion process to the solution (pre-formed ions) as was observed in the prior cVSSI studies³⁷.

It should be noted that the strongest association of ion intensity with $\log P$ for field-free cVSSI does not necessarily indicate that ions are produced via IEM. The earlier cVSSI work employing polar, protic solvent systems found that when there is not a sufficient electric field at the droplet surface to overcome the activation barrier, molecules will undergo ionization by the CRM similar to that proposed for sonic spray ionization³⁷. In end stages of CRM, the evaporating droplet will experience several fission events upon reaching the Rayleigh limit and will end with complete solvent evaporation and charge transfer to the analyte ion. It has been argued that even when CRM is the operative mechanism, under certain conditions, surface-active ions will be more favorably transferred to the smaller fission droplets, which will eventually allow their release to the gas-phase environment after complete solvent evaporation. So, a positive correlation with $\log P$ does not necessarily suggest that molecules in high organic content solvents and examined by field-free cVSSI cannot undergo CRM. Said differently, unlike in polar protic solvents (water and methanol), a correlation of $\log P$ with ion intensity might be more readily expected for field-free cVSSI even as the CRM is the operative process of ion production. Here the vicinity of the analyte to “protic agents” like H_3O^+ (generated from residual water) at the surface would facilitate ionization in the end stages of the droplet. For field-enabled conditions (field-enabled cVSSI and ESI) the shift in correlation with $\log P$ (direct to inverse) and PA provide some evidence for the IEM under wrong-way-round conditions as being the operative process.

In negative ion mode, the first correlations with pK_b are observed for the field-free cVSSI studies of neat ACN solutions (Table 2). Notably, these correlations are direct suggesting increased ionization for more acidic species as may be expected for negatively-charged ions. Thus it may be possible that there is sufficient residual water in neat ACN to produce some pre-formed ions. Admittedly, this is a relatively limited sample (15 compounds) and if only a few of these showed the ability to exist a pre-formed ions, this could shift the correlation as shown in Table 2. The strongest correlating factor for the neat ACN solutions for all three ionization sources is PA . Here, in contrast to positive ion mode studies, the correlations are inverse relationships. This is consistent with gas-phase deprotonation events as being the operative process. That said, as indicated in the discussion for the positive ion mode studies, such proton-transfer events could occur at the droplet surface or via reaction with gas-phase reagent ions. In negative ion mode, basic gas-phase species like OH^- or methoxide ion are

possible as a result of electric discharge.^{60 61 54} Additionally, it is noted that electrical breakdown is more readily observed at lower voltages for negative voltages and thus could argue for an APCI-like process being the primary mode upon application of voltage (field-enabled cVSSI and ESI).

When the solvent system became more protic (5% water) in nature an observed shift in the dominant correlations was observed (Table 2). For example, the ionization efficiency of all three ion modes shifted towards $\log P$ and PA . For ESI the $\log P$ correlation did not quite reach the confidence limits ($p = 0.06$). That said, it is essential to point out that the $\log P$ correlation for all three ionization techniques is positive, unlike that observed for the positive ion mode. Takayama and coworkers also reported a positive hydrophobicity correlation of amino acids dissolved in acetonitrile solvent systems under negative ion mode analysis.³⁵ This disparity between negative and positive mode $\log P$ correlation shows there could be an influence resulting from dielectric nature of the solvent with regard to positively- or negatively-charged analyte ions. Additionally, according to the IEM model proposed by Iribiane and Thomson, the rate of ion evaporation from the droplet depends on the solvation-free energy of the analyte and the surface electric field around the charged droplet.^{46 62} Therefore, the lower dielectric nature of ACN versus water could influence the free energy of solvation of anionic/ or cationic analytes differently.

Ion signal enhancement in field-free cVSSI in positive ion mode. A remarkable finding of the present work is the increase in average ion signal level obtained for 12 of the 17 compounds in positive ion mode when field-free cVSSI is employed compared to voltage-enabled techniques (Figure 1). Indeed, prior experimental and interpretive theoretical work suggests that solvents with lower surface tension and lower enthalpy of vaporization (surface tension; acetonitrile = 30 N/m water = 72 N/m, vaporization enthalpy; acetonitrile = 33 kJ/mol water = 44 kJ/mol) should more readily produce ions via the CRM.^{63 ,62} The positive ion studies presented here support this idea of highly efficient droplet drying for ACN.

A question then arises as to why the production of ions in negative ion mode is so suppressed for field-free cVSSI (Figure 3). That is, if droplet drying is so efficient for compounds in ACN, why are so few ions produced in negative ion mode? A possible answer to this question can be formulated when considering the production of negatively-charged ions by the field-enabled sources. Here, ion production is remarkably efficient as the upper range in ion signal level is higher by nearly an order of magnitude compared to the generation of ions by field-enabled sources in positive ion mode. As it is largely indicated by the multiple regression analysis, ions are produced by gas-phase proton transfer either at the droplet surface or via reagent ions. Because, electrical breakdown occurs at a lower negative bias compared with positive voltage, it can be argued that a much greater number of reagent ions may be produced for gas-phase proton transfer reactions. As it is assumed that the CRM is operative for field-free cVSSI in both positive and negative ion mode (see discussion above), it would also be argued that the

final transfer of charge during the droplet drying process was more efficient for positive ion mode than for negative ion mode. Whether or not this resulted from the selection of compounds for the study presented here cannot be determined from such limited sample sets.

Conclusions

The ion intensities of various small-molecule compounds have been reported for three different ionization techniques: field-free capillary vibrating sharp-edge ionization (cVSSI), field-enabled cVSSI, and ESI. Experiments have been conducted for samples dissolved in neat acetonitrile and 95% acetonitrile (5% water) under both positive and negative ion modes. Multiple regression analysis has been used to determine the degree to which different physicochemical characteristics of the molecule can be associated with the overall ionization efficiency in both positive and negative ion mode and to reveal how such associations can be different from aprotic to protic solvent conditions.

In general, for samples using an aprotic solvent having lower surface tension and low vaporization enthalpy, the log of the partition coefficient ($\log P$) is observed to correlate most significantly under field-free cVSSI conditions. This suggests ionization via the CRM as has been proposed for other field-free ionization sources. For both field-enabled cVSSI and ESI, $\log P$ and proton affinity (PA) are strongly associated with the ion intensities. Comparatively, in prior experiments, the log of the base dissociation constant (pK_b) has shown a much more significant correlation with protic solvents like water and methanol. This suggests that for the aprotic, polar solvent ACN, when an electric field is employed (field-enabled cVSSI and ESI), pre-formed ions are not responsible for the observed ion signals. Rather, gas-phase proton transfer reactions either at the droplet surface or via collisions with reagent ions occurs.

The differences in ionization efficiency observed suggest an opportunity to tailor ion source mode with desired analyte detection. For example, it may be most beneficial to use an aprotic solvent under field-free cVSSI conditions for certain molecules in positive ion mode. Conversely, for other compounds, it may be most beneficial to use field-enabled cVSSI in negative ion mode to gain the signal advantage produced by the cVSSI-APCI-like process. In any case, the new ionization techniques offer a number of possible usages and will require many more studies to begin to pin down their optimal operation under various conditions.

Acknowledgments

We are grateful for support of this work by the National Institutes of Health (R01GM135432)

Notes

The authors declare the following competing financial interest: S.J.V. has co-founded a start-up company, Invibragen Inc., to commercialize technologies involving vibrating sharp-edge spray ionization (VSSI).

References

- (1) Fenn, J. B.; Mann, M.; Meng, C. K.; Wong, S. F.; Whitehouse, C. M. Electrospray Ionization for Mass-Spectrometry of Large Biomolecules. *Science* **1989**, *246* (4926), 64-71. DOI: DOI 10.1126/science.2675315.
- (2) Tanaka, K.; Waki, H.; Ido, Y.; Akita, S.; Yoshida, Y.; Yoshida, T.; Matsuo, T. Protein and polymer analyses up to m/z 100 000 by laser ionization time-of-flight mass spectrometry. *Rapid Communications in Mass Spectrometry* **1988**, *2* (8), 151-153. DOI: 10.1002/rcm.1290020802.
- (3) Laiko, V. V.; Baldwin, M. A.; Burlingame, A. L. Atmospheric pressure matrix-assisted laser desorption/ionization mass spectrometry. *Anal Chem* **2000**, *72* (4), 652-657. DOI: 10.1021/ac990998k.
- (4) Emmett, M. R.; Caprioli, R. M. Micro-electrospray mass spectrometry: Ultra-high-sensitivity analysis of peptides and proteins. *J Am Soc Mass Spectrom* **1994**, *5* (7), 605-613. DOI: 10.1016/1044-0305(94)85001-1.
- (5) Wilm, M.; Mann, M. Analytical properties of the nanoelectrospray ion source. *Anal Chem* **1996**, *68* (1), 1-8. DOI: 10.1021/ac9509519.
- (6) Takats, Z.; Wiseman, J. M.; Gologan, B.; Cooks, R. G. Mass spectrometry sampling under ambient conditions with desorption electrospray ionization. *Science* **2004**, *306* (5695), 471-473. DOI: 10.1126/science.1104404.
- (7) Cody, R. B.; Laramée, J. A.; Durst, H. D. Versatile new ion source for the analysis of materials in open air under ambient conditions. *Anal Chem* **2005**, *77* (8), 2297-2302. DOI: 10.1021/ac050162j.
- (8) Horning, E.; Horning, M.; Carroll, D.; Dzidic, I.; Stillwell, R. New picogram detection system based on a mass spectrometer with an external ionization source at atmospheric pressure. *Analytical Chemistry* **1973**, *45* (6), 936-943.
- (9) Brown, H.; Oktem, B.; Windom, A.; Doroshenko, V.; Evans-Nguyen, K. Direct Analysis in Real Time (DART) and a portable mass spectrometer for rapid identification of common and designer drugs on-site. *Forensic Chemistry* **2016**, *1*, 66-73. DOI: <https://doi.org/10.1016/j.forc.2016.07.002>.
- (10) Bruno, A. M.; Cleary, S. R.; O'Leary, A. E.; Gizzi, M. C.; Mulligan, C. C. Balancing the utility and legality of implementing portable mass spectrometers coupled with ambient ionization in routine law enforcement activities. *Analytical Methods* **2017**, *9* (34), 5015-5022, 10.1039/C7AY00972K. DOI: 10.1039/C7AY00972K.
- (11) Lawton, Z. E.; Traub, A.; Fatigante, W. L.; Mancias, J.; O'Leary, A. E.; Hall, S. E.; Wieland, J. R.; Oberacher, H.; Gizzi, M. C.; Mulligan, C. C. Analytical Validation of a Portable Mass Spectrometer Featuring Interchangeable, Ambient Ionization Sources for High Throughput Forensic Evidence Screening. *Journal of the American Society for Mass Spectrometry* **2017**, *28* (6), 1048-1059. DOI: 10.1007/s13361-016-1562-2.
- (12) Meier, R. W. A field portable mass spectrometer for monitoring organic vapors. *American Industrial Hygiene Association Journal* **1978**, *39* (3), 233-239. DOI: 10.1080/0002889778507747.
- (13) Verbeck, G. F.; Bierbaum, V. M. Focus on Harsh Environment and Field-Portable Mass Spectrometry: Editorial. *Journal of the American Society for Mass Spectrometry* **2015**, *26* (2), 199-200. DOI: 10.1007/s13361-014-1057-y.
- (14) Hirabayashi, A.; Sakairi, M.; Koizumi, H. Sonic spray mass spectrometry. *Anal Chem* **1995**, *67* (17), 2878-2882. DOI: 10.1021/ac00113a023.
- (15) Wlekinski, M.; Li, Y.; Bag, S.; Sarkar, D.; Narayanan, R.; Pradeep, T.; Cooks, R. G. Zero Volt Paper Spray Ionization and Its Mechanism. *Anal Chem* **2015**, *87* (13), 6786-6793. DOI: 10.1021/acs.analchem.5b01225.
- (16) Song, L.; You, Y.; Evans-Nguyen, T. Surface Acoustic Wave Nebulization with Atmospheric-Pressure Chemical Ionization for Enhanced Ion Signal. *Anal Chem* **2019**, *91* (1), 912-918. DOI: 10.1021/acs.analchem.8b03927.

- (17) Pagnotti, V. S.; Chubatyi, N. D.; McEwen, C. N. Solvent assisted inlet ionization: an ultrasensitive new liquid introduction ionization method for mass spectrometry. *Anal Chem* **2011**, *83* (11), 3981-3985. DOI: 10.1021/ac200556z.
- (18) Chen, T.; Lin, J.; Chen, J.; Chen, Y. Ultrasonication-Assisted Spray Ionization Mass Spectrometry for the Analysis of Biomolecules in Solution. *Journal of the American Society For Mass Spectrometry* **2010**, *21* (9), 1547-1553, Article. DOI: 10.1016/j.jasms.2010.04.021.
- (19) Li, X.; Attanayake, K.; Valentine, S. J.; Li, P. Vibrating Sharp-edge Spray Ionization (VSSI) for voltage-free direct analysis of samples using mass spectrometry. *Rapid Commun Mass Spectrom* **2018**. DOI: 10.1002/rcm.8232.
- (20) Ranganathan, N.; Li, C.; Suder, T.; Karanji, A. K.; Li, X. J.; He, Z. Y.; Valentine, S. J.; Li, P. Capillary Vibrating Sharp-Edge Spray Ionization (cVSSI) for Voltage-Free Liquid Chromatography-Mass Spectrometry. *Journal of the American Society for Mass Spectrometry* **2019**, *30* (5), 824-831, Article. DOI: 10.1007/s13361-019-02147-0.
- (21) Li, C.; Attanayake, K.; Valentine, S. J.; Li, P. Facile Improvement of Negative Ion Mode Electrospray Ionization Using Capillary Vibrating Sharp-Edge Spray Ionization. *Anal Chem* **2020**, *92* (3), 2492-2502. DOI: 10.1021/acs.analchem.9b03983.
- (22) Kolakowski, B. A.; Grossert, J. S.; Ramaley, L. Studies on the positive-ion mass spectra from atmospheric pressure chemical ionization of gases and solvents used in liquid chromatography and direct liquid injection. *Journal of the American Society for Mass Spectrometry* **2004**, *15* (3), 311-324, Article. DOI: 10.1016/j.jasms.2003.10.019.
- (23) Narayanan, R.; Sarkar, D.; Cooks, R. G.; Pradeep, T. Molecular ionization from carbon nanotube paper. *Angew Chem Int Ed Engl* **2014**, *53* (23), 5936-5940. DOI: 10.1002/anie.201311053.
- (24) Pol, J.; Kauppila, T. J.; Haapala, M.; Saarela, V.; Franssila, S.; Ketola, R. A.; Kotiaho, T.; Kostianen, R. Microchip sonic spray ionization. *Anal Chem* **2007**, *79* (9), 3519-3523. DOI: 10.1021/ac070003v.
- (25) Yu, C.; Qian, X.; Chen, Y.; Yu, Q.; Ni, K.; Wang, X. Microfluidic self-aspiration sonic-spray ionization chip with single and dual ionization channels for mass spectrometry. *RSC Advances* **2016**, *6* (55), 50180-50189. DOI: 10.1039/c6ra07959h.
- (26) Mandra, V. J.; Kouskoura, M. G.; Markopoulou, C. K. Using the partial least squares method to model the electrospray ionization response produced by small pharmaceutical molecules in positive mode. *Rapid Commun Mass Spectrom* **2015**, *29* (18), 1661-1675. DOI: 10.1002/rcm.7263.
- (27) Ehrmann, B. M.; Henriksen, T.; Cech, N. B. Relative importance of basicity in the gas phase and in solution for determining selectivity in electrospray ionization mass spectrometry. *J Am Soc Mass Spectrom* **2008**, *19* (5), 719-728. DOI: 10.1016/j.jasms.2008.01.003.
- (28) Henriksen, T.; Juhler, R. K.; Svensmark, B.; Cech, N. B. The relative influences of acidity and polarity on responsiveness of small organic molecules to analysis with negative ion electrospray ionization mass spectrometry (ESI-MS). *J Am Soc Mass Spectrom* **2005**, *16* (4), 446-455. DOI: 10.1016/j.jasms.2004.11.021.
- (29) Oss, M.; Krueve, A.; Herodes, K.; Leito, I. Electrospray ionization efficiency scale of organic compounds. *Anal Chem* **2010**, *82* (7), 2865-2872. DOI: 10.1021/ac902856t.
- (30) Kiontke, A.; Oliveira-Birkmeier, A.; Opitz, A.; Birkemeyer, C. Electrospray Ionization Efficiency Is Dependent on Different Molecular Descriptors with Respect to Solvent pH and Instrumental Configuration. *PLoS One* **2016**, *11* (12), e0167502. DOI: 10.1371/journal.pone.0167502.
- (31) Liigand, J.; Laaniste, A.; Krueve, A. pH Effects on Electrospray Ionization Efficiency. *J Am Soc Mass Spectrom* **2017**, *28* (3), 461-469. DOI: 10.1007/s13361-016-1563-1.
- (32) Ikonomou, M. G.; Blades, A. T.; Kebarle, P. Electrospray-ion spray: a comparison of mechanisms and performance. *Analytical Chemistry* **1991**, *63* (18), 1989-1998. DOI: 10.1021/ac00018a017.
- (33) Zhou, S.; Hamburger, M. Effects of solvent composition on molecular ion response in electrospray mass spectrometry: Investigation of the ionization processes. *Rapid Communications in Mass Spectrometry* **1995**, *9* (15), 1516-1521, <https://doi.org/10.1002/rcm.1290091511>. DOI: <https://doi.org/10.1002/rcm.1290091511> (accessed 2022/04/19).
- (34) Schneider, R. P.; Lynch, M. J.; Ericson, J. F.; Fouda, H. G. Electrospray ionization mass spectrometry of semduramicin and other polyether ionophores. *Analytical Chemistry* **1991**, *63* (17), 1789-1794. DOI: 10.1021/ac00017a024.

- (35) Ami, Motoyama, A.; Takayama, M. Influence of Solvent Composition and Surface Tension on the Signal Intensity of Amino Acids in Electrospray Ionization Mass Spectrometry. *Mass Spectrometry* **2019**, *8*. DOI: 10.5702/massspectrometry.A0077.
- (36) Yao, Y.-N.; Wu, L.; Di, D.; Yuan, Z.-C.; Hu, B. Vibrating tip spray ionization mass spectrometry for direct sample analysis. *Journal of Mass Spectrometry* **2019**, *54*. DOI: 10.1002/jms.4429.
- (37) Jayasundara, K. U.; Li, C.; DeBastiani, A.; Sharif, D.; Li, P.; Valentine, S. J. Physicochemical Property Correlations with Ionization Efficiency in Capillary Vibrating Sharp-Edge Spray Ionization (cVSSI). *Journal of the American Society for Mass Spectrometry* **2021**, *32* (1), 84-94. DOI: 10.1021/jasms.0c00100.
- (38) Rossini, E.; Bochevarov, A. D.; Knapp, E. W. Empirical Conversion of pKa Values between Different Solvents and Interpretation of the Parameters: Application to Water, Acetonitrile, Dimethyl Sulfoxide, and Methanol. *ACS Omega* **2018**, *3* (2), 1653-1662. DOI: 10.1021/acsomega.7b01895.
- (39) Cech, N. B.; Enke, C. G. Relating electrospray ionization response to nonpolar character of small peptides. *Anal Chem* **2000**, *72* (13), 2717-2723. DOI: 10.1021/ac9914869.
- (40) Kiontke, A.; Billig, S.; Birkemeyer, C. Response in Ambient Low Temperature Plasma Ionization Compared to Electrospray and Atmospheric Pressure Chemical Ionization for Mass Spectrometry. *Int J Anal Chem* **2018**, *2018*, 5647536. DOI: 10.1155/2018/5647536.
- (41) Gamero-Castaño, M.; Fernandez de la Mora, J. Mechanisms of Electrospray Ionization of Singly and Multiply Charged Salt Clusters. *Analytica Chimica Acta* **2000**, *406*, 67-91. DOI: 10.1016/S0003-2670(99)00596-6.
- (42) Znamenskiy, V.; Marginean, I.; Vertes, A. Solvated Ion Evaporation from Charged Water Nanodroplets. *The Journal of Physical Chemistry A* **2003**, *107* (38), 7406-7412. DOI: 10.1021/jp034561z.
- (43) Kebarle, P.; Peschke, M. On the mechanisms by which the charged droplets produced by electrospray lead to gas phase ions. *Analytica Chimica Acta* **2000**, *406* (1), 11-35, Article. DOI: 10.1016/S0003-2670(99)00598-x.
- (44) Kebarle, P.; Verkerk, U. H. ELECTROSPRAY: FROM IONS IN SOLUTION TO IONS IN THE GAS PHASE, WHAT WE KNOW NOW. *Mass Spectrometry Reviews* **2009**, *28* (6), 898-917, Review. DOI: 10.1002/mas.20247.
- (45) Rohner, T. C.; Lion, N.; Girault, H. H. Electrochemical and theoretical aspects of electrospray ionisation. *Physical Chemistry Chemical Physics* **2004**, *6* (12), 3056-3068, Review. DOI: 10.1039/b316836k.
- (46) Iribarne, J. V. On the evaporation of small ions from charged droplets. *The Journal of Chemical Physics* **1976**, *64* (6). DOI: 10.1063/1.432536.
- (47) Tang, L.; Kebarle, P. DEPENDENCE OF ION INTENSITY IN ELECTROSPRAY MASS-SPECTROMETRY ON THE CONCENTRATION OF THE ANALYTES IN THE ELECTROSPRAYED SOLUTION. *Analytical Chemistry* **1993**, *65* (24), 3654-3668, Article. DOI: 10.1021/ac00072a020.
- (48) Dole, M.; Mack, L. L.; Hines, R. L. MOLECULAR BEAMS OF MACROIONS. *Journal of Chemical Physics* **1968**, *49* (5), 2240-&, Article. DOI: 10.1063/1.1670391.
- (49) Cech, N. B.; Krone, J. R.; Enke, C. G. Predicting Electrospray Response from Chromatographic Retention Time. *Analytical Chemistry* **2001**, *73* (2), 208-213. DOI: 10.1021/ac0006019.
- (50) Tang, L.; Kebarle, P. Effect of the conductivity of the electrosprayed solution on the electrospray current. Factors determining analyte sensitivity in electrospray mass spectrometry. *Analytical Chemistry* **1991**, *63* (23), 2709-2715. DOI: 10.1021/ac00023a009.
- (51) Kelly, M. A.; Vestling, M. M.; Fenselau, C. C.; Smith, P. B. Electrospray analysis of proteins. *A comparison of positive-ion and negative-ion mass spectra at high and low pH* **1992**, *27* (10), 1143-1147, Article. DOI: 10.1002/oms.1210271028.
- (52) Wang, G.; Cole, R. B. Disparity between solution-phase equilibria and charge state distributions in positive-ion electrospray mass spectrometry. *Organic Mass Spectrometry* **1994**, *29* (8), 419-427.
- (53) Mansoori, B. A.; Volmer, D. A.; Boyd, R. K. 'Wrong-way-round' Electrospray Ionization of Amino Acids. *Rapid Communications in Mass Spectrometry* **1997**, *11* (10), 1120-1130, [https://doi.org/10.1002/\(SICI\)1097-0231\(19970630\)11:10<1120::AID-RCM976>3.0.CO;2-Q](https://doi.org/10.1002/(SICI)1097-0231(19970630)11:10<1120::AID-RCM976>3.0.CO;2-Q). DOI: [https://doi.org/10.1002/\(SICI\)1097-0231\(19970630\)11:10<1120::AID-RCM976>3.0.CO;2-Q](https://doi.org/10.1002/(SICI)1097-0231(19970630)11:10<1120::AID-RCM976>3.0.CO;2-Q) (accessed 2022/04/19).
- (54) Zhou, S.; Cook, K. D. Protonation in electrospray mass spectrometry: Wrong-way-round or right-way-round? *Journal of the American Society for Mass Spectrometry* **2000**, *11* (11), 961-966. DOI: 10.1016/S1044-0305(00)00174-4.

- (55) Cole, R. B. *Electrospray ionization mass spectrometry : fundamentals, instrumentation, and applications*. 1997.
- (56) Kebarle, P. A brief overview of the present status of the mechanisms involved in electrospray mass spectrometry. *Journal of Mass Spectrometry* **2000**, 35 (7), 804-817, Article. DOI: 10.1002/1096-9888(200007)35:7<804::aid-jms22>3.0.co;2-q.
- (57) Pursell, M. E.; Sharif, D.; DeBastiani, A.; Li, C.; Majuta, S.; Li, P.; Valentine, S. J. Development of cVSSI-APCI for the Improvement of Ion Suppression and Matrix Effects in Complex Mixtures. *Analytical Chemistry* **2022**. DOI: 10.1021/acs.analchem.1c05136.
- (58) Kebarle, P.; Godbole, E. W. Mass-Spectrometric Study of Ions from the α -Particle Irradiation of Gases at Near Atmospheric Pressures. *The Journal of Chemical Physics* **1963**, 39 (4), 1131-1132. DOI: 10.1063/1.1734371 (accessed 2022/04/20).
- (59) Negative air ions created by water shearing improve erythrocyte deformability and aerobic metabolism. *Indoor Air* **2004**, 14 (4), 293-297, <https://doi.org/10.1111/j.1600-0668.2004.00254.x>. DOI: <https://doi.org/10.1111/j.1600-0668.2004.00254.x> (accessed 2022/06/27).
- (60) Harrison, A. G. *Chemical Ionization Mass Spectrometry*. 2 ed.; Routledge: New York, 1992; pp 91-100.
- (61) Bruins, A. P. Mass spectrometry with ion sources operating at atmospheric pressure. *Mass Spectrometry Reviews* **1991**, 10 (1), 53-77, <https://doi.org/10.1002/mas.1280100104>. DOI: <https://doi.org/10.1002/mas.1280100104> (accessed 2022/04/20).
- (62) Labowsky, M. A model for solvated ion emission from electrospray droplets. *Rapid Communications in Mass Spectrometry* **2010**, 24 (21), 3079-3091, <https://doi.org/10.1002/rcm.4738>. DOI: <https://doi.org/10.1002/rcm.4738> (accessed 2022/04/20).
- (63) Nguyen, S.; Fenn John, B. Gas-phase ions of solute species from charged droplets of solutions. *Proceedings of the National Academy of Sciences* **2007**, 104 (4), 1111-1117. DOI: 10.1073/pnas.0609969104 (accessed 2022/04/20).
- (64) D.C., B. *Experimentation: An Introduction to Measurement Theory and Experiment Design*; Benjamin Cummings, 1994.

Figure captions

Figure 1. Bar diagram of log of the ion signal intensities of each analyte molecule in neat acetonitrile under positive ion mode, Field-free cVSSI, Field-enabled cVSSI, ESI. Blue bars represent Field-free cVSSI, orange bars represent Field-enabled cVSSI and grey bars represent cESI. Error bars represent relative error of one standard deviation about the mean⁶⁴.

Figure 2. Bar diagram log of the ion signal intensities of each analyte molecule in 95% acetonitrile under Field-free cVSSI, Field-enabled cVSSI, ESI. Blue bars represent Field-free cVSSI, orange bars represent Field-enabled cVSSI and grey bars represent cESI. Error bars represent relative error of one standard deviation about the mean⁶⁴.

Figure 3. Bar diagram of log of the ion signal intensities of each analyte molecule in neat acetonitrile under negative ion mode Field-free cVSSI, Field-enabled cVSSI, ESI. Blue bars represent Field-free cVSSI, orange bars represent Field-enabled cVSSI and grey bars represent cESI. Error bars represent relative error of one standard deviation about the mean⁶⁴.

Figure 4. Bar diagram of log of the ion signal intensities of each analyte molecule in 95% acetonitrile under Field-free cVSSI, Field-enabled cVSSI, ESI. Blue bars represent Field-free cVSSI, orange bars represent Field-enabled cVSSI and grey bars represent cESI. Error bars represent relative error of one standard deviation about the mean⁶⁴.

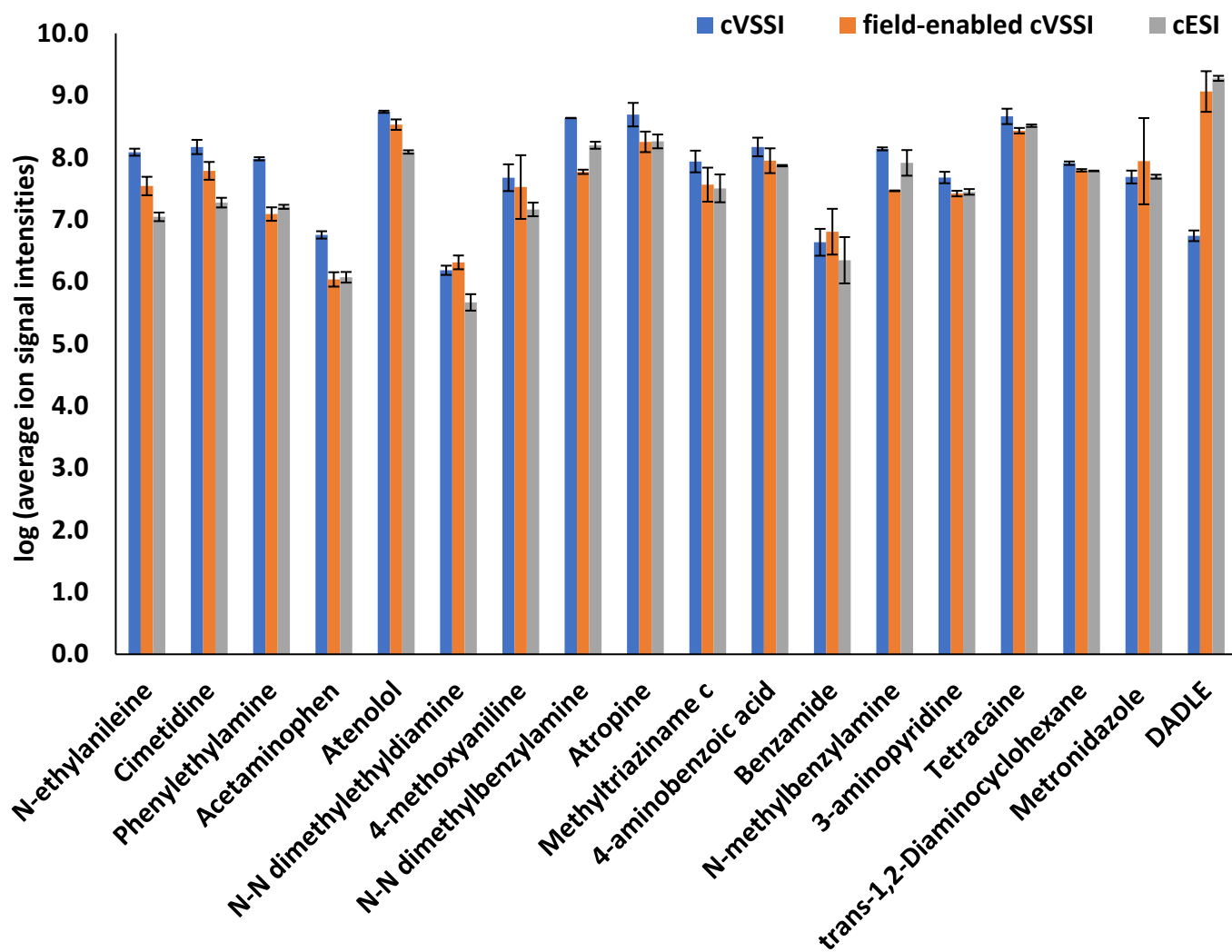


Figure 1

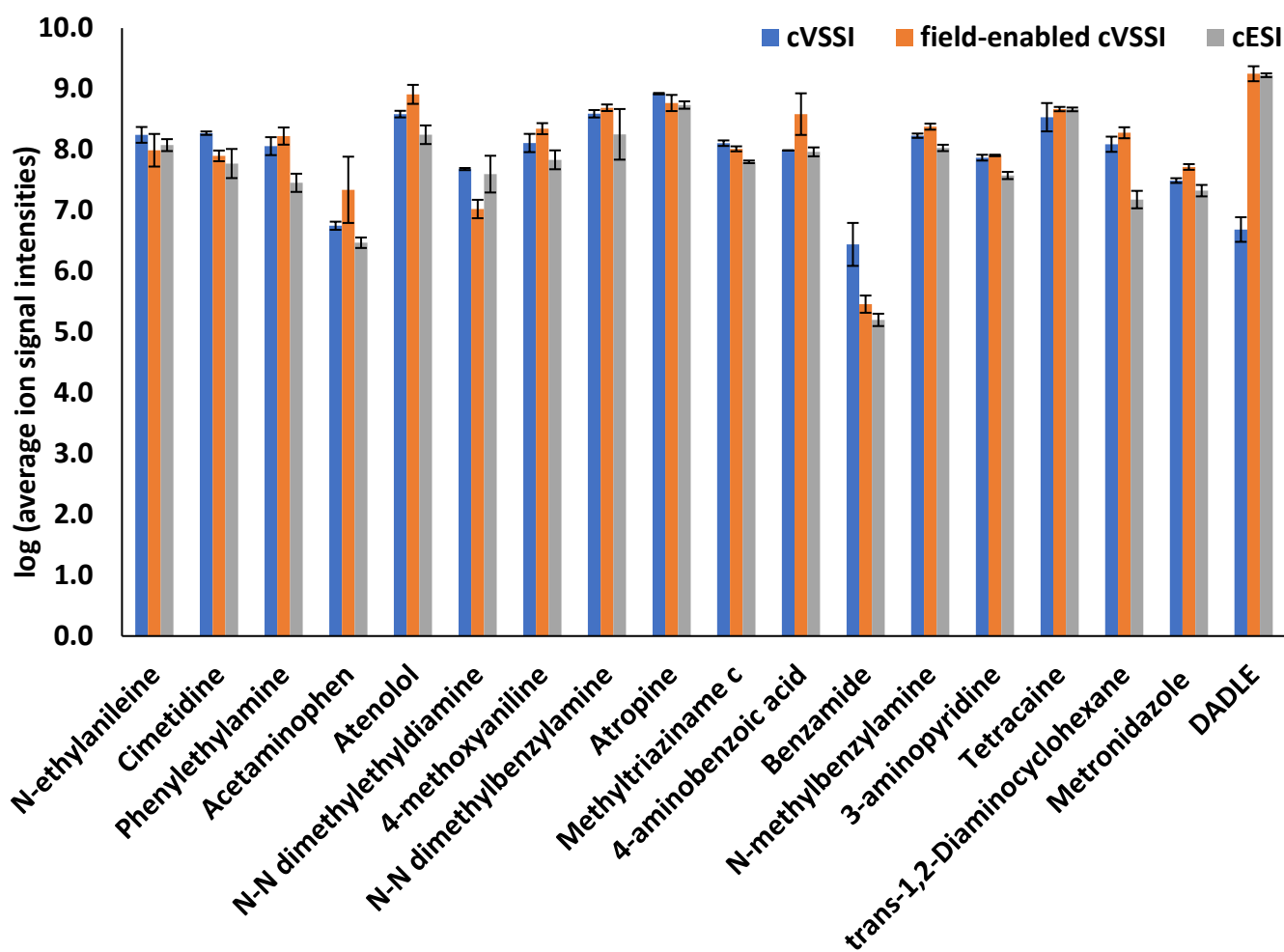


Figure 2

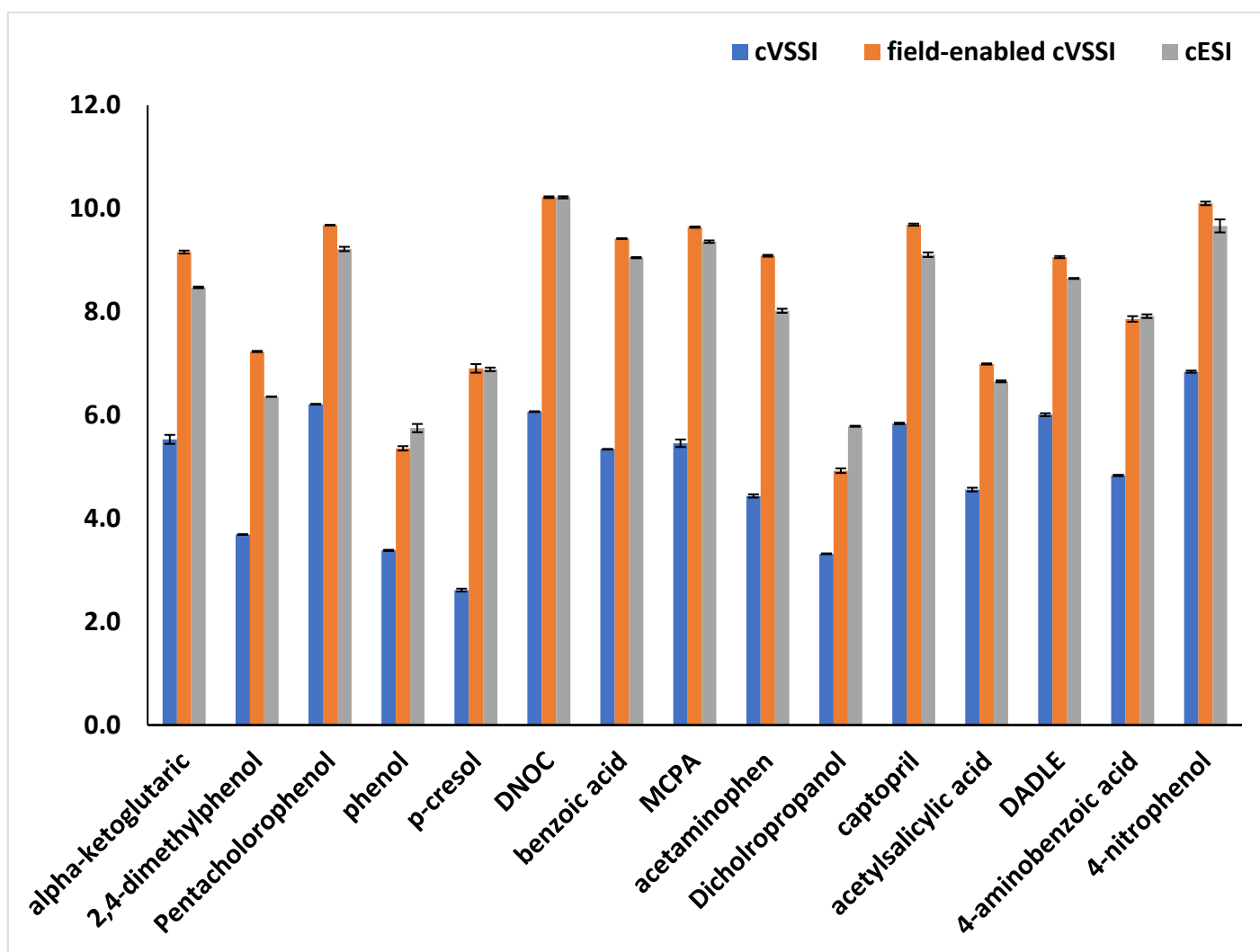


Figure 3

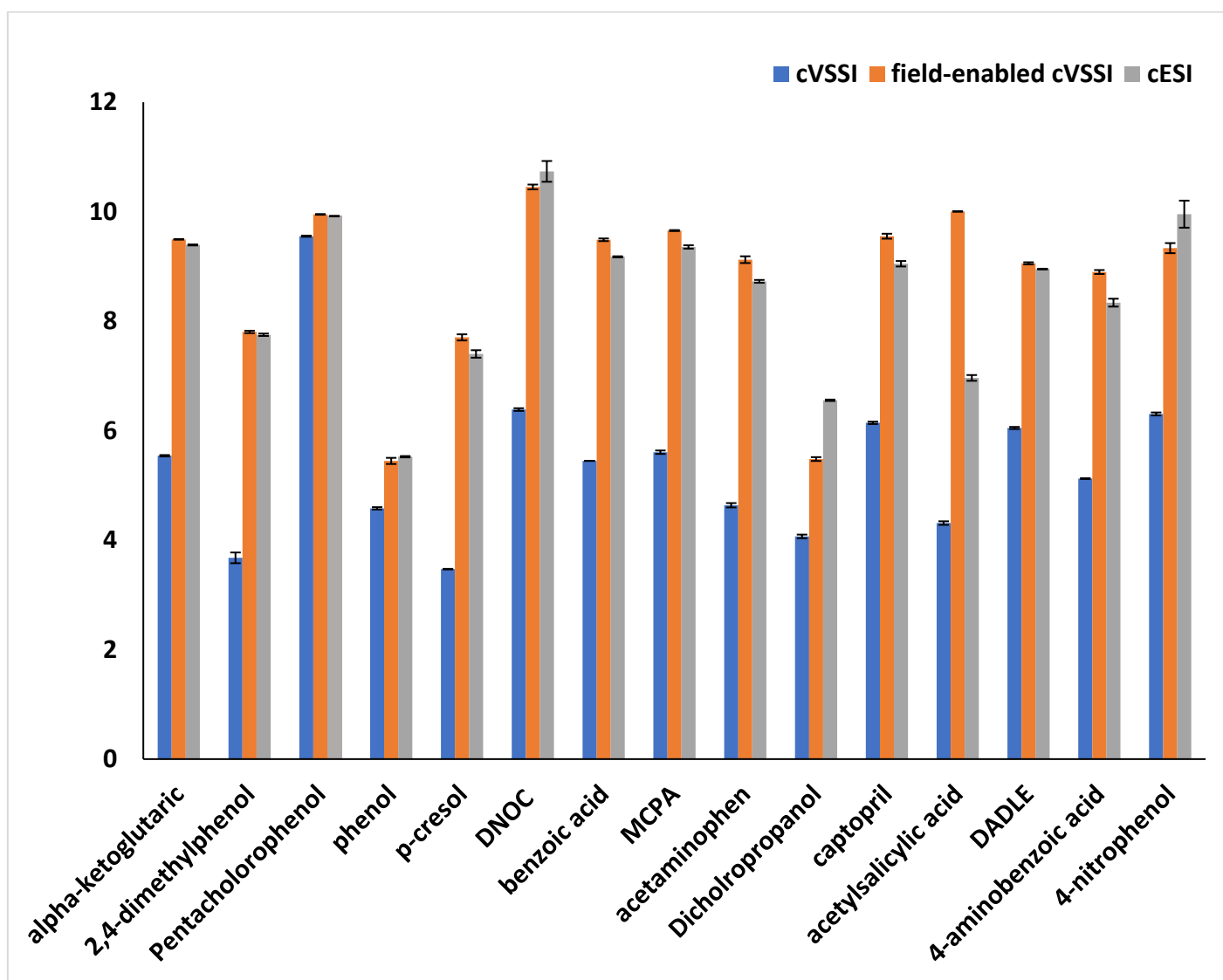


Figure 4

Property ^a	Neat acetonitrile (positive mode)			95% acetonitrile (positive mode)		
	cVSSI ^b	cVSSI+2KV	ESI	cVSSI	cVSSI+2KV	ESI
pk _b	-0.175(0.235) ^c	0.166 (0.395)	0.235 (0.235)	-0.163 (0.340)	0.107(0.582)	0.264(0.146)
logP	0.235 (<0.001)	-0.319 (0.024)	-0.387(0.004)	0.434(<0.001)	-0.215(0.117)	-0.278(0.031)
PA	0.269 (0.073)	0.519 (0.011)	0.639 (<0.001)	0.257(0.257)	0.539(0.008)	0.721(<0.001)

Table 1. Beta coefficients and the associated significance values for the positive mode.

Properties	Neat acetonitrile (negative mode)			95% acetonitrile (negative mode)		
	cVSSI	cVSSI+2KV	ESI	cVSSI	cVSSI+2KV	ESI
pk _b	0.525(0.001)	0.352(0.031)	0.243(0.161)	0.070(0.630)	-0.295(0.082)	-0.388(0.021)
logP	-0.066(0.605)	0.071(0.585)	0.128(0.364)	0.587(<0.001)	0.317(0.025)	0.230(0.060)
PA	-0.791(<0.001)	-0.759(<0.001)	-0.625(<0.001)	-0.527(<0.001)	-0.388(0.019)	-0.766(<0.001)

Table 2. Beta coefficients and the associated significance values for the negative mode.

^aPhysicochemical property for the different compounds. The compound-specific values are listed in Table S1/S2 in the Supporting Information section.

^bIonization mode. cVSSI, cVSSI+2kV, and ESI correspond to the Field-free cVSSI, Field-enabled cVSSI, and ESI experiments, respectively. See the Experimental section for more details.

^cBeta coefficients and associated significance values (given parenthetically) for the separate regression analyses. Bolded values represent the most significant results for each experiment. The sign of the coefficient indicates the nature of the correlation (positive versus negative correlation).

Supporting Information

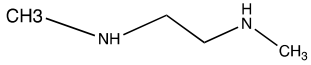
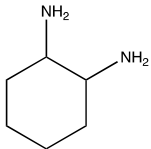
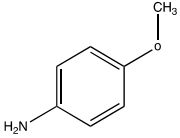
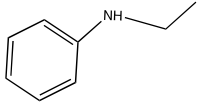
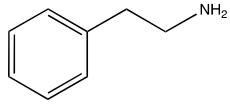
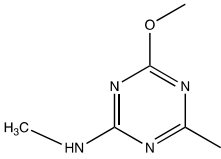
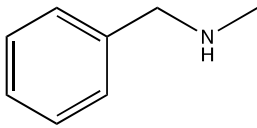
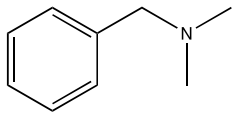
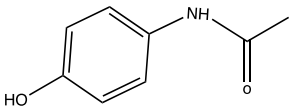
Table S1. Structures and physicochemical property values for the compounds used in the positive mode ionization experiments.

Table S2. Structures and physicochemical property values for the compounds used in the negative mode ionization experiments.

Table S3 (a,b). Molecule-specific ion intensities for the neat acetonitrile and 95% acetonitrile in positive mode analysis

Table S4 (a,b). Molecule-specific ion intensities for the neat acetonitrile and 95% acetonitrile in positive mode analysis

Table S1

Compound	Structure	pKa		pKb (CH ₃ CN)	logP	PA (kJ/mol)	MW
		Water	CH ₃ CN				
N,N dimethylethyldiamine		9.48	11.71	20.49	-0.60	937.4	88.15
Trans-1,2-Diaminocyclohexane		9.9	17.69	14.51	-0.008	973.5	114.19
4-methoxyaniline		5.36	12.16	20.04	0.74	900.3	123.15
N-ethylaniline		4.91	11.71	20.49	2.13	924.8	121.14
Phenylethylamine		9.79	17.49	14.71	1.49	936.2	121.18
Methyltriazinamine c		4.87	12.57	19.63	-1.34	882.7	154.17
N-methylbenzylamine		9.41	17.31	14.89	1.6	980.4	121.80
N-N-dimethylbenzylamine		8.9	17.75	14.45	1.98	968.4	135.17
Acetaminophen		-4.4	2.4	29.8	0.907	824.1	151.17

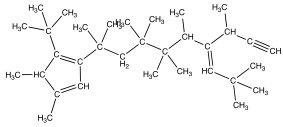
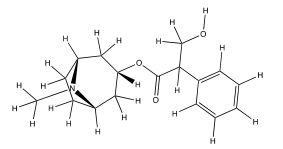
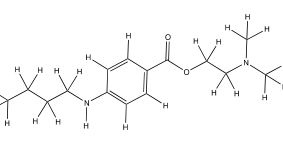
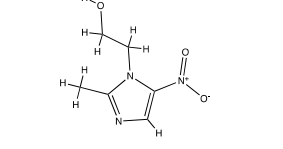
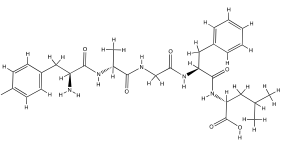
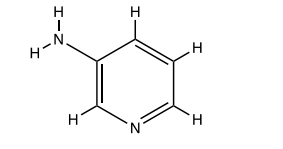
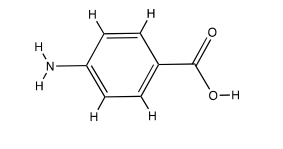
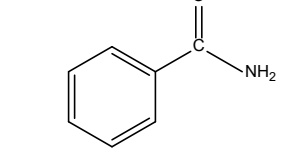
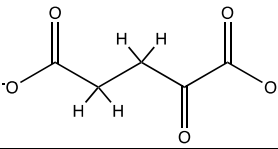
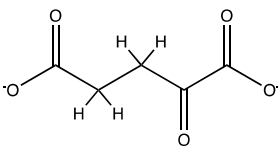
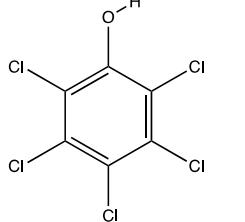
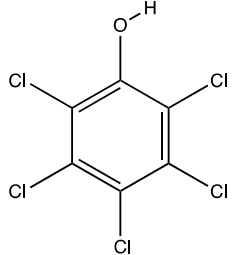
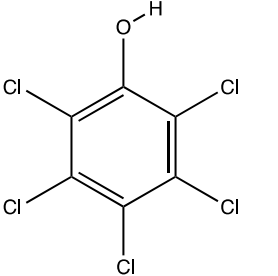
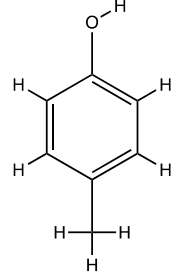
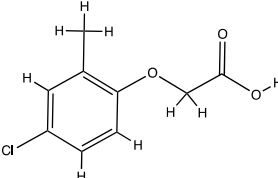
Cimetidine		6.91	13.51	18.69	-0.109	992.5	252.34
Atropine		9.39	17.69	14.51	1.57	1002.1	289.37
Tetracaine		8.42	16.72	15.48	2.80	1024.4	264.36
Metronidazole		3.03	17.23	14.97	-0.46	886.9	171.10
DADLE		7.73	15.43	16.77	-1.30	1008.6	569.60
3-aminopyridine		5.75	13.45	18.75	-0.07	957.6	94.10
4-aminobenzoic acid		2.69	9.49	22.71	0.80	834.5	137.10
Benzamide		-1.2	-	-	0.74	892.1	121.05

Table S2

#	Compound	Structure	pKa		logP	PA (kJ/mol)	MW
			Water	CH ₃ CN			
1	alpha-ketoglutaric		2.66	18.16	-0.10	1355.78	146.10
2	2,4-dimethylphenol		10.71	27.01	2.4	1448.24	122.16
3	Pentachlorophenol		4.98	21.38	4.69	1316.37	266.34
4	phenol		10.02	26.32	1.48	1432.65	94.11
5	p-cresol		10.36	26.66	1.94	1439.48	108.14
6	benzoic acid		4.08	19.58	1.89	1411.05	122.10
7	MCPA		3.36	18.86	2.49	1373.64	200.62

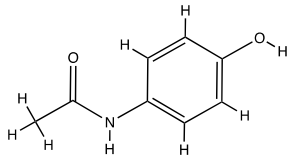
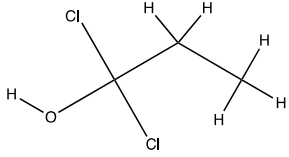
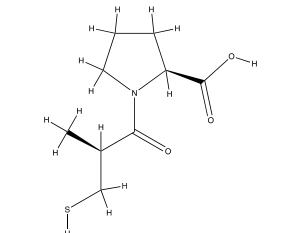
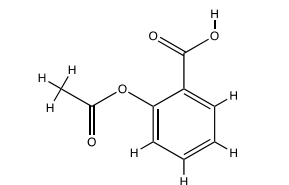
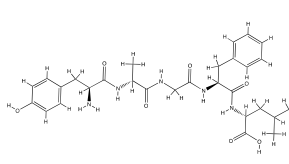
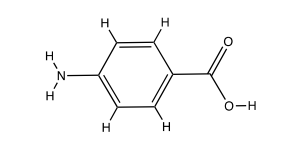
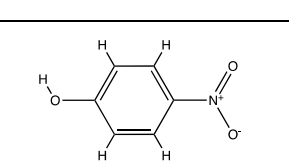
8	acetaminophen		9.46	25.76	0.90	1400.93	151.17
9	Dichloropropanol		2.95	18.45	3.07	1376.90	235.06
10	captopril		4.02	19.52	0.72	1373.18	217.00
11	acetylsalicylic acid		3.41	18.91	1.23	1372.95	180.10
12	DADLE		3.70	19.2	-1.3	1342.43	569.60
13	4-aminobenzoic acid		4.77	20.27	0.80	1431.87	137.10
14	4-nitrophenol		7.07	23.37	1.61	1341.69	139.10

Table S3 (a)

#	Compound	Neat acetonitrile solvent system					
		cVSSI		cVSSI+2KV		ESI	
		[M+H] ⁺	S.D.	[M+H] ⁺	S.D.	[M+H] ⁺	S.D.
1	N,N dimethylethyldiamine	1.53E+06	2.62E+05	2.05E+06	5.26E+05	4.65E+05	1.42E+05
2	Trans-1,2-Diaminocyclohexane	8.11E+07	5.20E+06	6.23E+07	2.81E+06	6.09E+07	7.09E+05
3	4-methoxyaniline	4.74E+07	2.36E+07	3.35E+07	3.96E+07	1.46E+07	3.69E+06
4	N-ethylaniline	1.22E+08	1.59E+07	3.48E+07	1.19E+07	1.11E+07	1.78E+06
5	Phenylethylamine	9.55E+07	5.61E+06	1.23E+07	3.08E+06	1.61E+07	1.22E+06
6	Methyltriazinamine c	8.64E+07	3.48E+07	3.66E+07	2.31E+07	3.19E+07	1.65E+07
7	N-methylbenzylamine	1.38E+08	7.57E+06	2.91E+07	1.93E+07	8.21E+07	3.90E+07
8	N-N-dimethylbenzylamine	4.33E+08	2.62E+05	2.05E+06	5.26E+05	4.65E+05	1.42E+05
9	Benzamide	4.32E+06	2.15E+06	6.40E+06	5.44E+06	2.22E+06	1.91E+06
10	Acetaminophen	5.68E+06	7.73E+05	1.09E+06	4.48E+07	1.18E+06	2.33E+05
11	Cimetidine	1.48E+08	3.92E+07	6.11E+07	7.04E+07	1.88E+07	3.38E+06
12	Atropine	4.91E+08	2.15E+08	1.79E+08	7.66E+07	1.82E+08	4.66E+07
13	Tetracaine	4.60E+08	1.31E+08	2.71E+08	1.36E+08	3.26E+08	1.50E+07
14	Metronidazole	4.86E+07	1.16E+07	8.75E+07	7.59E+08	4.92E+07	3.60E+06
15	DADLE	5.49E+06	1.09E+06	1.16E+09	1.01E+09	1.89E+09	1.76E+08
16	3-aminopyridine	4.77E+07	1.01E+07	2.63E+07	5.85E+07	2.80E+07	2.92E+06

17	4-aminobenzoic acid	1.48E+08	5.12E+07	8.89E+07	2.25E+07	7.40E+07	1.85E+06
18	Atenolol	5.46E+08	2.20E+07	3.39E+08	6.58E+07	1.23E+08	7.64E+06

Table S3(b)

#	Compound	95% acetonitrile solvent system					
		cVSSI		cVSSI+2KV		ESI	
		[M+H] ⁺	S.D.	[M+H] ⁺	S.D.	[M+H] ⁺	S.D.
1	N,N dimethylethyldiamine	4.80E+07	1.93E+06	1.06E+07	3.70E+06	3.97E+07	2.76E+07
2	Trans-1,2-Diaminocyclohexane	1.23E+08	3.54E+07	1.90E+08	3.96E+07	1.51E+07	5.00E+06
3	4-methoxyaniline	1.29E+08	4.46E+07	2.22E+08	4.63E+07	6.82E+07	2.44E+07
4	N-ethylaniline	1.75E+08	5.24E+07	9.79E+07	6.06E+07	1.19E+08	2.69E+07
5	Phenylethylamine	1.14E+08	3.89E+07	1.68E+08	5.46E+07	2.85E+07	9.83E+06
6	Methyltriazinamine c	1.28E+08	1.35E+07	1.03E+08	9.81E+06	6.32E+07	3.11E+06
7	N-methylbenzylamine	1.70E+08	1.40E+07	2.40E+08	2.77E+07	1.07E+08	1.29E+07
8	N-N-dimethylbenzylamine	3.90E+08	5.52E+07	4.90E+08	6.10E+07	1.79E+08	1.72E+08
9	Benzamide	2.77E+06	2.25E+06	2.88E+05	9.40E+04	1.59E+05	3.71E+04
10	Acteaminophen	5.61E+06	8.64E+05	2.19E+07	2.75E+07	2.95E+06	5.86E+05
11	Cimetidine	1.87E+08	1.22E+07	7.91E+07	1.60E+07	5.92E+07	3.27E+07
12	Atropine	8.36E+08	2.15E+07	5.87E+08	1.80E+08	5.43E+08	7.63E+07
13	Tetracaine	3.42E+08	1.84E+08	4.66E+08	3.82E+07	4.60E+08	3.25E+07
14	Metronidazole	3.11E+07	2.75E+06	5.20E+07	5.61E+06	2.12E+07	4.60E+06
15	DADLE	4.86E+06	2.27E+06	1.78E+09	5.05E+08	1.68E+09	1.20E+08
16	3-aminopyridine	7.40E+07	8.16E+06	8.05E+07	2.29E+06	3.77E+07	5.16E+06

17	4-aminobenzoic acid	9.74E+07	4.95E+05	3.85E+08	3.04E+08	9.22E+07	1.56E+07
18	Atenolol	3.85E+08	4.82E+07	8.14E+08	2.93E+08	1.76E+08	6.22E+07

Table S4 (a)

#	Compound	Neat acetonitrile solvent system					
		cVSSI		cVSSI+2KV		ESI	
		[M-H] ⁻	S.D.	[M-H] ⁻	S.D.	[M-H] ⁻	S.D.
1	alpha-ketoglutaric	3.40E+05	1.18E+05	1.44E+09	1.63E+08	2.98E+08	1.91E+07
2	2,4-dimethylphenol	4.89E+03	3.54E+01	1.71E+07	8.08E+05	2.28E+06	1.53E+04
3	Pentachlorophenol	1.63E+06	4.73E+04	4.79E+09	5.77E+07	1.65E+09	2.80E+08
4	phenol	2.41E+03	1.08E+02	2.28E+05	3.87E+04	5.62E+05	1.79E+05
5	p-cresol	4.10E+02	4.58E+01	8.04E+06	2.67E+06	7.71E+06	1.06E+06
6	DNOC	1.17E+06	7.27E+08	1.66E+10	1.08E+09	1.65E+10	1.31E+09
7	benzoic acid	2.19E+05	5.51E+03	2.62E+09	7.57E+07	1.12E+09	4.93E+07
8	MCPA	2.86E+05	8.34E+04	4.38E+09	2.11E+08	2.29E+09	2.15E+08
9	acetaminophen	2.73E+04	3.46E+03	1.22E+09	8.74E+07	1.05E+08	1.65E+07
10	Dichloropropanol	2.07E+03	6.43E+01	8.41E+04	1.48E+04	6.10E+05	2.31E+04
11	captopril	6.92E+05	3.91E+04	4.89E+09	3.91E+08	1.28E+09	2.29E+08
12	acetylsalicylic acid	3.62E+04	5.23E+03	9.79E+06	4.64E+05	4.51E+06	3.30E+05
13	DADLE	1.02E+06	1.17E+05	1.15E+09	9.54E+07	4.44E+08	1.63E+07

14	4-aminobenzoic acid	6.81E+04	3.23E+03	7.29E+07	1.57E+07	8.26E+07	1.16E+07
15	4-nitrophenol	6.95E+06	5.98E+05	1.26E+10	1.74E+09	4.62E+09	2.32E+09

Table S4 (b)

#	Compound	95% acetonitrile solvent system					
		cVSSI		cVSSI+2KV		ESI	
		[M-H] ⁻	S.D.	[M-H] ⁻	S.D.	[M-H] ⁻	S.D.
1	alpha-ketoglutaric	3.48E+05	1.75E+04	3.12E+09	5.20E+07	2.47E+09	9.02E+07
2	2,4-dimethylphenol	4.75E+03	1.86E+03	6.37E+07	5.51E+06	5.65E+07	4.90E+06
3	Pentachlorophenol	3.57E+09	1.51E+08	8.93E+09	2.19E+08	8.31E+09	8.62E+07
4	phenol	3.81E+04	3.30E+03	2.80E+05	6.27E+04	3.34E+05	1.61E+04
5	p-cresol	2.95E+03	6.36E+01	5.06E+07	1.13E+07	2.52E+07	6.88E+06
6	DNOC	2.43E+06	2.35E+05	2.83E+10	4.95E+09	5.45E+10	4.13E+10
7	benzoic acid	2.81E+05	1.73E+03	3.07E+09	2.95E+08	1.50E+09	5.77E+07
8	MCPA	4.04E+05	5.06E+04	4.52E+09	1.63E+08	2.27E+09	2.77E+08
10	acetaminophen	4.34E+04	6.83E+03	1.33E+09	3.27E+08	5.34E+08	5.53E+07
11	Dichloropropanol	1.17E+04	1.54E+03	3.03E+05	4.22E+04	3.59E+06	1.83E+05
12	captopril	1.39E+06	1.19E+05	3.57E+09	6.40E+08	1.12E+09	2.23E+08
13	acetylsalicylic acid	2.05E+04	2.64E+03	1.01E+10	2.38E+08	9.19E+06	1.93E+06

14	DADLE	1.12E+06	8.50E+04	1.14E+09	8.72E+07	8.95E+08	2.34E+07
15	4-aminobenzoic acid	1.33E+05	2.65E+03	7.91E+08	1.14E+08	2.18E+08	6.26E+07
16	4-nitrophenol	2.02E+06	2.19E+05	2.16E+09	7.94E+08	9.02E+09	8.90E+09